Atomically resolved study of initial stages of hydrogen etching and adsorption on GaAs(110)

D. S. Rosenzweig [*] and M. N. L. Hansemann
Institut für Festkörperphysik, Technische Universität Berlin, 10623 Berlin, Germany

M. Schnedler and Ph. Ebert
Ernst Ruska-Centrum (ER-C-1) and Peter Grünberg Institut (PGI-5), Forschungszentrum Jülich GmbH, 52425 Jülich, Germany

H. Eisele
Institut für Physik, Otto-von-Guericke Universität Magdeburg, 39106 Magdeburg, Germany

(Received 31 October 2022; accepted 16 December 2022; published 27 December 2022)

The initial stages of hydrogen adsorption on GaAs(110) surfaces at room temperature are investigated by atomically resolved scanning tunneling microscopy and spectroscopy. Two effects are found to occur simultaneously: On the one hand a surface phase separation occurs, creating 1×1 reconstructed fully hydrogen-covered areas while leaving the surface in between completely hydrogen free. In the fully hydrogen-covered areas, hydrogen bonds equally to As- and Ga-derived dangling bonds, unbuckling and passivating the surface. On the other hand, hydrogen-induced point defects are formed with increasing density. The dominating defects consist of As vacancy–hydrogen defect complexes, formed by preferential hydrogen etching of As. Using a defect-molecule model the Ga-H bridge bonds and double-occupied Ga dangling bonds are suggested to be at the origin of the observed surface Fermi level pinning 0.25 to 0.3 eV above the valence band edge, identical within error margins for *p*- and *n*-doped GaAs(110).

DOI: 10.1103/PhysRevMaterials.6.124603

I. INTRODUCTION

Hydrogen is the most common impurity in epitaxial growth of semiconductors. On the one hand, hydrogen is applied as carrier gas and molecular component of the precursors in metal organic chemical vapor epitaxy (MOCVD) and its variants [1,2]. On the other hand, hydrogen is used for cleaning [3] and passivation [4] of semiconductor surfaces. Furthermore, hydrogen is present as residual gas in every ultrahigh vacuum system used to grow, pattern, and contact semiconductor devices [5,6]. Therefore, a detailed understanding of the atomic interaction mechanisms of hydrogen with semiconductor surfaces is crucial for optimization, particularly of semiconductor nanostructures, due to their large surface to bulk ratio. At present, compound semiconductor nanoscale structures are of highest interest, since their electronic properties can be tuned by alloying without detrimental effects of lattice mismatch and strain, suppressing dislocation formation [7–9]. Such nanostructures exhibit mostly low-energy nonpolar facets, i.e., (110) surfaces in the case of zinc-blende III–V semiconductors [10–12].

For hydrogen interaction with GaAs(110) two different effects are reported in the literature: On the one hand, hydrogen adsorbs to the As and Ga dangling bonds, passivating them [13–16]. On the other hand, a surface dissociation process leads to Ga-rich surfaces [13,17]. Thus far, it is debated under which conditions (i.e., atomic hydrogen fraction and dose) which of the two effects dominates, since all experimental methods used up to now [14,17,18] only probe integral information and lack atomic resolution. Theory only addresses the ideal surfaces without decomposition processes [16,19].

In this paper we investigate the interaction of hydrogen with GaAs(110) surfaces as model system using atomically resolved scanning tunneling microscopy (STM) and spectroscopy (STS). We focus on the initial stages (<1 L) of hydrogen adsorption at room temperature. We identify a passivation of GaAs(110) surfaces by hydrogen bonding simultaneously to As- and Ga-derived dangling bonds as well as the concomitant formation of a high density of hydrogen-etching-induced point defects, consisting primarily of As vacancy–hydrogen defect complexes. The Ga-H bridge bonds and the double-occupied Ga dangling bonds within the defects are proposed to be at the origin of the observed surface Fermi level pinning about 0.25 to 0.3 eV above the valence band edge and essentially identical for *n*- and *p*-doped GaAs(110).

II. EXPERIMENTAL

For the experiments we used *n*- and *p*-type GaAs wafers with Si and Zn doping concentrations of nominally 2.0×10^{18} and 1.0×10^{18} cm^{-3}, respectively. Samples cut from the wafers are cleaved under ultrahigh vacuum conditions ($<2\times10^{-8}$ Pa) to obtain atomically clean (110) surfaces, which are investigated by STM and STS in the as-cleaved as well as hydrogen-exposed state. All measurements are performed at room temperature (300 K) with tungsten tips.

[*] dorothee.rosenzweig@physik.tu-berlin.de

 ©2022 American Physical Society

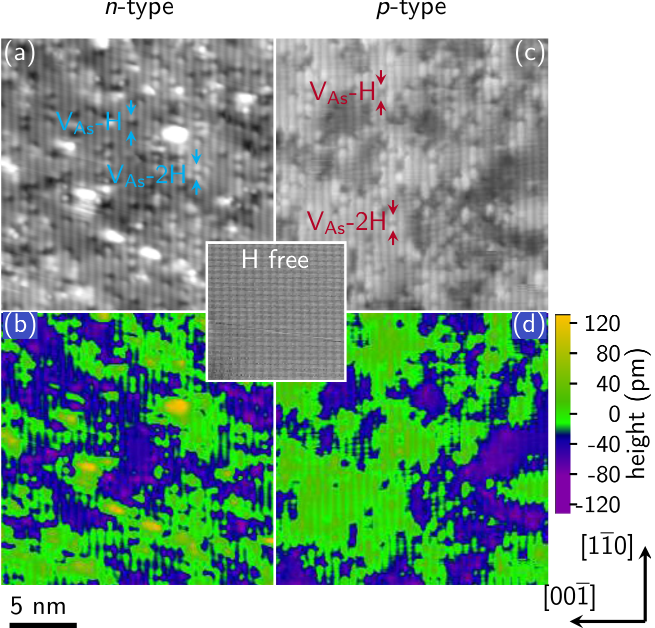

FIG. 1. Atomically resolved constant-current STM images of the (a), (b) *n*- and (c), (d) *p*-doped GaAs(110) surfaces after 0.5 L hydrogen exposure (acquired at set points of $V_S = -1.8$ V, $I_T = 50$ pA and $V_S = -2.0$ V, $I_T = 50$ pA, respectively). (b) and (d) represent false-color images of (a) and (c), respectively, illustrating a phase separation characterized by slightly lowered (bluish) and elevated (greenish) areas. The height difference between those areas is about 40 pm. Inset: Atomically resolved constant-current STM image of the GaAs(110) surface without hydrogen exposure. The arrows in (a) and (c) mark defects, further analyzed using height profiles in Fig. 2.

The atomic hydrogen is provided by a hydrogen atom beam source (Dr. Eberl MBE-Komponenten GmbH HABS) with a cracking efficacy of about 98%, being much larger than in all previous investigations [13–18]. The samples are exposed to the atomic hydrogen beam for about one second, at comparable hydrogen partial pressures. Unfortunately, the partial pressure in the atomic hydrogen beam is not directly measurable. Hence, the flux can only be determined afterward on the basis of the surface changes. This yields hydrogen exposures of approximately 0.5 L for each exposure assuming a sticking coefficient of atomic hydrogen of almost 1.

III. RESULTS

A. *n*-type GaAs(110)

The freshly cleaved clean *n*-type GaAs(110) surfaces exhibit large atomically flat terraces with the typical 1×1 surface relaxation (see, e.g., inset of Fig. 1) [20–24]. On the terraces only a few defects occur, which can be assigned to Si dopants and thermally formed Ga surface vacancies (V_{Ga}) [25,26]. On the basis of the doping level, the given temperature, and the time after cleavage, the dopant and vacancy concentrations are estimated to be typically in the range of 2×10^{11} cm^{-2} and 1×10^{12} cm^{-2}, respectively [27].

Upon hydrogen exposure the *n*-type GaAs(110) surface structure changes drastically: (i) The 1×1 surface separates in two phases, which are distinguishable by a difference in height. (ii) A high concentration of As vacancy–related defects is formed. (iii) A Fermi level shift occurs upon hydrogen adsorption.

The first two effects are illustrated in Fig. 1(a), which shows a constant-current STM image obtained after 0.5 L atomic hydrogen exposure:

(i) In the STM image one can observe atomic rows along the [1$\bar{1}$0] direction running from top to bottom, in analogy to the clean GaAs(110) surface (see inset). The contrast visible as atomic rows arises from electrons tunneling out of the occupied dangling bonds localized above the As surface atoms. The local height of these atomic rows appears to split up into areas with slightly higher (brighter contrast) and lower (darker contrast) heights. The height difference between the two types of areas is approximately 40 pm. For better visibility, Fig. 1(b) shows a false-color representation of the STM image of Fig. 1(a). The greenish areas correspond to the areas 40 pm higher than the bluish ones. The false-color STM image reveals a size for types of domains of approximately 10–20 nm^2. Upon further hydrogen exposure, the area fraction of domains with lower height increases from 43% to 58% for hydrogen exposures of 0.5 to 0.67 L.

(ii) In addition, a large concentration of point defects occurs in both phases after hydrogen exposure. Besides a few white protrusions attributed to adatoms, the dominating types of defects contain each one missing an As-derived dangling bond. These defects can be further distinguished by the contrast of the adjacent lattice sites along the atomic rows: The basic defect has no brighter or darker contrast of the neighboring lattice sites of the missing dangling bond. As elaborated in the discussion section, this defect is attributed to a single arsenic surface vacancy and is hence labeled V_{As} [24,28].

Two other types of defects differ from the isolated V_{As} by exhibiting either one or two brighter contrasts on the adjacent As lattice sites, labeled V_{As}-H and V_{As}-2H, respectively. This can be observed in the line profiles along the atomic rows in Figs. 2(a) and 2(b), respectively, as well as in the enlarged STM images (see insets). Furthermore, the height profiles reveal in the case of V_{As}-H that the single brighter dangling bond is centered on top of the adjacent As lattice site, whereas in the case of V_{As}-2H the two brighter dangling bonds are shifted inward into the vacancy site by approximately $0.3\ \frac{a_0}{\sqrt{2}}$.

Figure 3(a) illustrates the measured concentrations of the various observed defects vs hydrogen exposure. On the clean *n*-type GaAs(110) surface without hydrogen exposure only V_{Ga} exists. The rather small V_{Ga} concentration is essentially independent of the hydrogen exposure. In contrast, all As vacancy–related defects occur only after hydrogen exposure and appear to reach a saturation level at 0.5 L hydrogen exposure already.

(iii) Figures 4(a) and 4(b) provide a comparison of tunnel spectra on the *n*-type GaAs(110) surface before (a) and after hydrogen exposure of 0.5 L (b). Without hydrogen, the onset voltages of the positive and negative branches of the tunnel spectrum are close to the Fermi level at 0 V, with no apparent band gap. As outlined below this agrees with an unpinned

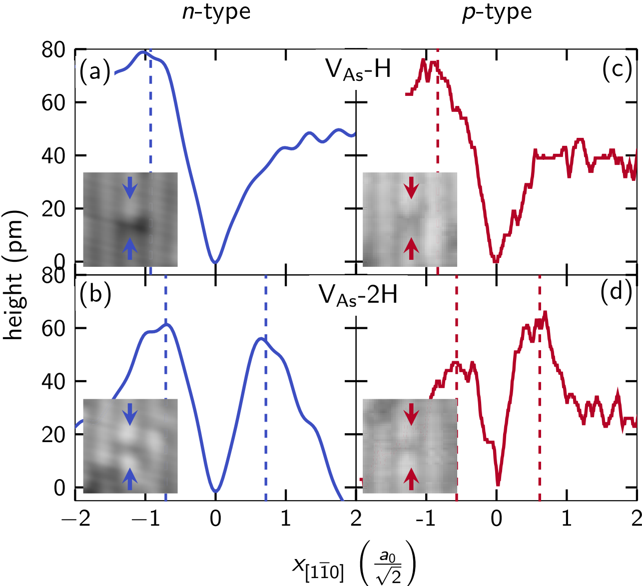

FIG. 2. Height profiles along the [1$\bar{1}$0] direction through the V_{As}-H (top) and V_{As}-2H (bottom) defects marked in Fig. 1 for (a), (b) *n*- and (c), (d) *p*-type GaAs(110) surfaces after hydrogen exposure. Dashed vertical lines mark the positions of the filled dangling bonds above the neighboring As atoms. For the V_{As}-2H defects, the profiles indicate an inward displacement of the neighboring As atoms. The insets illustrate STM images of the corresponding defects.

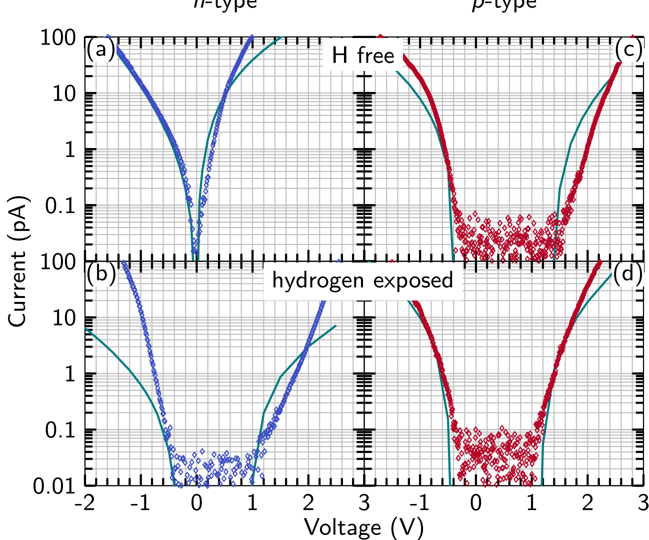

FIG. 4. Scanning tunneling current spectra of the *n*- [(a), (b)] and *p*-type [(c), (d)] GaAs(110) surfaces in the hydrogen-free state (top) and after hydrogen exposure of (b) 0.5 L and (d) 0.67 L (bottom). The experimental data, shown as symbols, have been acquired at tip-sample separations fixed at set currents of 50 pA at (a), (c), (d) −1.4 V and (b) −1.2 V. Self-consistent simulations are illustrated as lines.

n-type doped GaAs surface [30]. With 0.5 L hydrogen exposure, the tunnel spectrum exhibits a clear band gap and the onsets of the both current branches are shifted away from the Fermi level to −0.4 V and +1 V. Hence, hydrogen exposure creates a surface, which exhibits more *p*-type characteristics. As outlined below, this is induced by a Fermi level pinning by defects. Upon further hydrogen exposure, the spectra do effectively not change anymore corroborating a saturation with defects.

B. *p*-type GaAs(110)

The STM images of the hydrogen-exposed *p*-type GaAs(110) surface [Figs. 1(c) and 1(d)] reveal almost identical structural changes to those for *n*-type GaAs. (i) The 1×1 relaxed surface separates again into two phases distinguishable by different height. (ii) A high concentration of V_{As}-related defects is formed. These defects can be again classified using the contrast at the adjacent As lattice sites along the atomic rows:

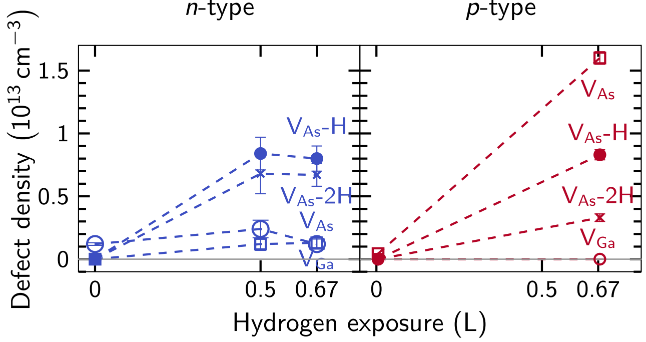

FIG. 3. Concentration of the various observed defects on (a) *n*-type and (b) *p*-type GaAs(110) vs hydrogen exposure. The data at 0 L exposure correspond to the hydrogen-free cleavage surfaces, extracted from prior measurements [27,29].

On clean *p*-type GaAs(110) surfaces only single missing As-derived dangling bonds can be observed. The defect has no adjacent brighter dangling bonds and has been shown previously to be an arsenic surface vacancy (labeled V_{As}) [31–33]. The single arsenic vacancies may form thermally by Langmuir desorption, even without any hydrogen exposure [34]. In contrast to clean *n*-type GaAs(110) surfaces, no V_{Ga} are detected on clean as well as on hydrogen exposed *p*-type surfaces.

Upon hydrogen exposure two further defects appear on *p*-type surfaces, in analogy to *n*-type surfaces: The defects exhibit one (two) brighter contrasts on the adjacent As lattice sites of the missing As-derived dangling bond [see Figs. 2(c) and 2(d) and the respective insets, labeled V_{As}-H and V_{As}-2H]. The spatial shifts of the adjacent brighter maxima agree also with those observed on *n*-type GaAs(110) surfaces upon hydrogen exposure. The observed defect concentrations are given in Fig. 3(b). Note that higher single As vacancy concentrations are induced by hydrogen on *p*-type surfaces as compared to *n*-type surfaces. No V_{Ga} appear after hydrogen exposure.

Finally, Figs. 4(c) and 4(d) illustrate that the tunnel spectra of *p*-type GaAs(110) before and after hydrogen exposure are rather similar in terms of current onsets and Fermi level position. They differ by a larger apparent band gap for hydrogen-free surfaces as compared with hydrogen-exposed

surfaces. With hydrogen exposure the onset voltages of the two current branches are almost identical to those found on *n*-type surfaces [compare Fig. 4(b) with Fig. 4(d)].

IV. DISCUSSION

The experimental results demonstrate three effects of hydrogen exposure onto GaAs(110) surfaces: (i) The surface undergoes a phase separation, leading to two types of domains, differing in their height. (ii) A variety of point defects form, which are related to missing As, independent of the type of doping. (iii) A shift of the Fermi level occurs upon hydrogen exposure, primarily for *n*-type GaAs(110).

A. Hydrogen on the defect-free surface

The observation of two phases with 40 pm height difference (i.e., only ≈20% of the monolayer thickness) can be understood by a simultaneous presence of hydrogen-covered and hydrogen-free GaAs(110) surface areas: Since the fraction of the phase with lower height increases with hydrogen exposure, it can be attributed to a fully hydrogen-covered 1×1 surface. The phase with higher height corresponds then to GaAs(110) surface areas without adsorbed hydrogen [green in Figs. 1(b) and 1(d)].

The facts that the 1×1 unit cell persists in both phases and that the height difference is much smaller than the thickness of an atomic layer indicate that hydrogen leads to a different relaxation of the surface atoms as compared with the clean surface.

Indeed, LEED [17] and grazing incidence x-ray diffraction (GIXD) [35] found that a hydrogen coverage debuckles the GaAs(110) surface. Theoretical calculations predict that hydrogen binds to the filled and empty dangling bonds above the As and Ga surface atoms [36–38]. This yields As-H and Ga-H bonds whose energies are shifted close to the valence band maximum [39–41]. These bonds exhibit an sp^3-type (re)hybridization favoring a tetrahedral coordination of the surface atoms. Hence, the buckling of the clean surface is removed. In fact, the buckling is even slightly reversed [35,42]. This debuckling lowers the position of the As surface atoms by approximately 30 pm relative to the As surface positions on the clean hydrogen-free surface. It can be anticipated that the length (i.e., the extent of the density of states into the vacuum) of the filled dangling bond above an As atom (hydrogen-free surface) and that of the As-H bond derived from this dangling bond are almost identical. Hence, the downward shift of the As atom translates rather directly into a reduced height of the hydrogen-covered surface [relative to hydrogen-free GaAs(110)].

The fact that two types of domains with and without hydrogen form indicates an attractive hydrogen-hydrogen interaction on GaAs(110). This can be understood in terms of charge neutrality: If a hydrogen atom bonds individually to only one As (or Ga) surface atom, it needs to repel the excess (or attract the lacking) electron. This would create a charge build-up, which can be avoided by passivating adjacent As and Ga dangling bonds with an additional bound hydrogen. This interpretation is further supported by the fact that *p*-type GaAs(110) surfaces exhibit the very same phase separation as on the *n*-type material.

B. Defects

The point defects observed on the freshly cleaved clean surfaces and those on the hydrogen exposed surfaces differ quite considerably. First we discuss the point defects on the freshly cleaved surfaces, followed by those after hydrogen exposure.

1. Clean, hydrogen-free surfaces

After cleavage we observed missing As dangling bonds on the *p*-type GaAs(110) surface and two brighter nearest-neighboring As dangling bonds on the *n*-type GaAs(110) surface. These defects were investigated previously in detail and attributed to single As surface vacancies (*p*-type) and Ga surface vacancies (*n*-type) [26,31,43]. They form spontaneously at room temperature by Langmuir desorption and represent the intrinsic defects of the GaAs(110) surface [26,34,44].

2. Defects induced by hydrogen exposure

Upon hydrogen exposure, the types of point defects and their concentrations change drastically. The newly formed point defects consist always of a single missing As dangling bond, typically in conjunction with one or two brighter appearing adjacent As dangling bonds. These defects form upon hydrogen exposure independently of the type of doping of the GaAs(110) surface, in contrast to the above-discussed intrinsic defects of the clean surfaces. The missing As dangling bond can be assigned to the presence of an As vacancy in analogy to the intrinsic defects on clean surfaces. If the missing As dangling bond would arise from a single hydrogen bonded to an As dangling bond, it would also appear like a vacancy [45]. However, the fact that the defects occur on both phases of the hydrogen-exposed GaAs(110) surface (i.e., fully hydrogen-covered and hydrogen-free phases) rules out a single bonded hydrogen as the origin of the missing As dangling bond. As a side note, therefore, hydrogen bonded to surface atoms is also not giving rise to the intrinsic vacancies observed on freshly cleaved clean surfaces without intentional hydrogen exposure, excluding the suggestion of Ref. [45]. Hence, the As vacancy–related defects, formed during hydrogen exposure, can be considered as residues from As surface atoms removed by interaction with hydrogen atoms. The etching process can be anticipated to lead to arsine desorption from the GaAs(110) surface.

The preferential formation of As vacancies shifts the surface stoichiometry toward a Ga-rich surface upon on hydrogenation. This observation is corroborated by PES, EELS, and mass spectrometry measurements, which find a Ga-rich surface and mostly As desorption upon hydrogen exposure [15,46].

Next we address the existence of different configurations of As vacancy–related defects formed by hydrogen exposure (see Fig. 2) The concentrations of the defects labeled V_{As}-H and V_{As}-2H are found to increase with hydrogen exposure. Thus,

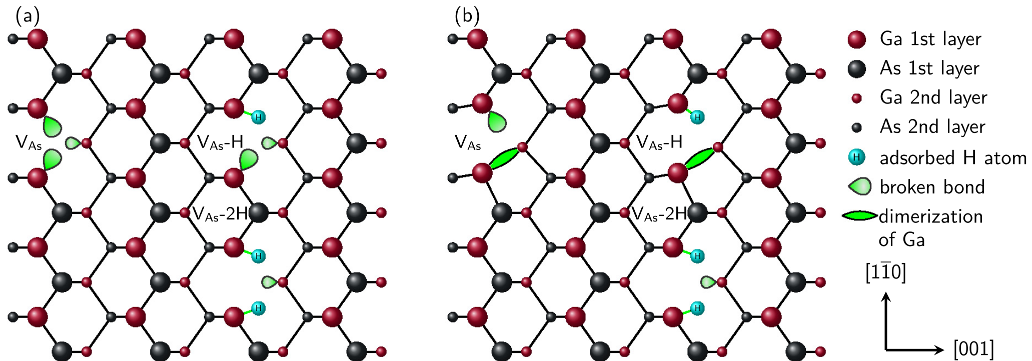

FIG. 5. Schematic illustrating the defect-molecule model discussion of the single As vacancy V_{As} as well as hydrogen vacancy defect complexes (V_{As}-H and V_{As}-2H). (a) Upon vacancy formation, three bonds are broken, leaving behind two broken bridge bonds and one broken back bond. (b) The broken bonds rehybridize and form defect states and/or interact with one or more hydrogen atoms.

the defects contain hydrogen atoms. In order to elucidate the structure we turn to a defect-molecule model approach.

The removal of a surface As atom leads to three broken bonds attached at the adjacent Ga atoms [see V_{As} in Fig. 5(a)]. Using a defect-molecule model, these dangling bonds rehybridize and form three defect states, one in the valence band, in the band gap, and in the conduction band, each. Note that since the same types of defects occur in both the hydrogen-covered and hydrogen-free surface phases, we only consider the dangling bonds within the vacancy and their interaction with hydrogen atoms. In the presence of hydrogen, additional hydrogen atoms can bond to the broken bonds in the vacancy. For example, one hydrogen atom can saturate the broken (bridge) bond of an adjacent surface Ga atom [see V_{As}-H in Fig. 5(a)]. One can anticipate that the saturated Ga prefers a planar configuration, lifting the (1$\bar{1}$0) mirror symmetry [see schematic of V_{As}-H complex in Fig. 5(b)]. The remaining two broken bonds (bridge and back bonds) can be expected to rehybridize in analogy to step edges, resulting in a brighter contrast of the adjacent As atoms [47,48]. Similarly, the two broken bridge bonds of the adjacent Ga surface atoms can be saturated by hydrogen atoms (see V_{As}-2H in Fig. 5). This preserves the (1$\bar{1}$0) mirror symmetry and equally affects both neighboring As atoms (V_{As}-2H complex in Fig. 5). Note that hydrogen can in principle also bond to the broken back bond of the second-layer Ga atom. However, this cannot be observed in STM images, since the tip-sample separation is about 2 Å larger than for Ga-H bridge bonds, reducing the tunnel current accordingly. The exact rehybridization and relaxation can only be determined on the basis of DFT calculations. The here outlined As vacancy–hydrogen complexes agree well with the observation of three dominating point defects formed on hydrogen-exposed n- and p-type GaAs(110) surfaces and reproduce/explain their symmetry and appearance in STM images well.

At this stage we differentiate the defect complexes formed by hydrogen from previously observed defect complexes. Some prior found defects (vacancy-dopant complexes [26,49–51], Schottky defects [52,53]) have a similar appearance of one bright dangling bond adjacent to a vacancy. However, vacancy-dopant complexes can be excluded as they exist in any orientation unlike the here observed defect being always aligned along the atomic rows. Schottky defects can be ruled out, as they can only account for a single bright neighboring As dangling bond, but not for defects with two. In addition, these defects would not account for the hydrogen exposure dependence. Hence, the defects observed here were not found on any III–V semiconductor (110) surfaces previously.

C. Fermi level pinning

The As vacancy–hydrogen complexes can be anticipated to have localized defect levels in analogy to those of an isolated As vacancy. These will influence the position of the Fermi level at the surface and thereby modulate the tunneling spectra. As outlined in the experimental results above, the spectra change rather subtly only for p-type GaAs(110) during hydrogen exposure, whereas the changes on n-GaAs(110) are quite pronounced in terms of onset voltages and apparent band gap.

In order to understand this behavior we simulated the tunnel current following a two-step method [54,55]: First, the electrostatic potential as well as the charge carrier distributions of the tip-vacuum-semiconductor system in thermal equilibrium are self-consistently derived using finite differences. Second, the one-dimensional electrostatic potential along the central axis through the tip apex is used to derive the tunnel currents through the vacuum barrier in a WKB approximation–based model described in Refs. [56,57].

As parameters we have to consider the charge-transfer levels and concentrations of the point defects. The charge-transfer level of an ensemble of a defect is modeled as a Gaussian-shaped surface-charge distribution 0.1 eV wide. The Gaussian charge distribution arises from the convolution of a sharp charge-transfer level with the Fermi function at room temperature. The possible electron occupation (i.e., integral of Gaussian charge distribution) is given by the density of defects.

1. n-type GaAs(110)

The spectrum of the hydrogen-free n-doped surface, shown in Fig. 4(a), exhibits apparently no band gap. This arises from the tip-induced downward band bending at negative voltages, creating an electron accumulation in the conduction band. From the accumulation zone electrons tunnel into the tip

even at very small applied negative voltages, resulting in an onset of the negative current branch close to 0 V. Tunneling from filled valence band states occurs only at much larger negative voltages around -1.5 to -2 V and only shows up in a change of slope (not visible in the voltage range shown). The current at positive voltages arises from tunneling into empty conduction band states, starting close to 0 V, too, due to the n-type doping of the material. The corresponding tunnel current simulation [lines in Fig. 4(a)] agrees with the experimentally measured spectrum (symbols), corroborating the presence on an essentially unpinned hydrogen-free n-type surface. Note that we estimated that the density of V_{Ga} defects at the acquisition time of the spectrum 26.5 h after cleavage at 300 K is 1×10^{12} cm^{-2} [27,28]. This concentration is too small to lead to a Fermi level pinning at the voltages used, although a weak pinning (i.e., band bending) is present even without a tunneling tip present above the surface.

After hydrogen exposure the spectra change fundamentally. No current is any longer observed within the fundamental band gap and the voltage separation of the onsets of the positive and negative current branches corresponds to the band gap. In addition the Fermi level is found to be shifted toward the valence band edge. This indicates a pinning, which can be attributed to arise from the high point defect densities observed in the STM images [Fig. 1(a)]. The solid line in Fig. 4(b) shows the simulation assuming a full pinning by a defect density of 2.0×10^{13} cm^{-2} with a charge-neutrality level near the valence band edge E_V and a $(0/-)$ charge-transfer level at $E_V + 0.3$ eV, a tip work function of 4.5 eV, and radius of 100 nm. The simulated current onsets agree well with those measured, corroborating the defect-induced pinning in the lower part of the band gap upon hydrogen exposure.

2. *p*-type GaAs(110)

Second, we turn to p-type GaAs(110) without hydrogen exposure. The spectra were acquired 6 h after cleavage at room temperature. After this time the density of As vacancies formed by Langmuir desorption is still very low (1.0×10^{10} cm^{-2} range) and has no effect on the Fermi level position.

The solid line in Fig. 4(c) illustrates the tunnel current calculated for an unpinned p-type GaAs(110) surface. A good agreement is found with the measured current values. At negative voltages tunneling out of filled valence band states occurs. At positive voltages no tunneling into the tip-induced hole accumulation zone in the valence band is detected, since the tunneling barrier is larger than for tunneling into the conduction band states, which starts at about 1.5–1.6 V. Therefore, a clear voltage range with no detectable current exists, larger than the fundamental band gap due to tip-induced band bending. Hence, the spectrum reveals an unpinned p-doped GaAs(110) surface.

After hydrogen exposure of p-type GaAs(110) a large defect density is present. These defects have charge-transfer levels within the band gap, which lead to a pinning of the Fermi level. We used the energy position of the charge-transfer level as fit parameter, to simulate the tunnel current. The best simulation is achieved for an energy position of the $(+/0)$ charge-transfer level of $E_V + (0.25 \pm 0.1)$ eV (and a charge-neutrality level above the charge-transfer level), a tip work function of 4.65 eV, and radius of 10 nm. The good agreement indicates that the surface is essentially fully pinned by defects, which were formed by hydrogen exposure.

3. *Microscopic origin of the Fermi level pinning*

Now, we address the physical origin of the Fermi level pinning on basis of a defect-molecule model discussion of the observed defects. First, we consider p-type GaAs(110). The dominating defect observed is the single As vacancy [Fig. 3(b)]. The lowest charge-transfer level of the As vacancy is the $(+/0)$ charge-transfer level, which is calculated to be 0.49 eV above the valence band in the *GW* approximation reproducing the experimental band gap very well [58]. DFT calculations with the LDA approximation [59–61] underestimate the energy position and hence cannot be taken into account [58]. Experimentally we find a charge transition level of $(E_V + 0.25) \pm 0.1$ eV above E_V. This value is too low to be in accordance with that of the As vacancy. Thus, the As vacancy is unlikely to provide the lowest charge-transfer level (closest to E_F) on p-type GaAs(110) after hydrogen exposure. Thus, we turn to the vacancy-hydrogen complexes. As outlined above with the help of the defect-molecule model, the binding of a hydrogen atom to a broken bridge bond of one of the adjacent Ga atoms leads to a Ga-H bond and a rehybridization of the two broken bonds at the remaining adjacent surface and second-layer Ga atoms [see schematic structure of V_{As}-H complex in Fig. 5(b)]. This Ga-Ga bond occurs also in the single positively charged arsenic vacancy and its energy is in the valence band [see V_{As} in Fig. 5(b)] [33]. Hence, the only defect state in the valence band of the V_{As}-H complex arises from the Ga-H bridge bond. Note that this needs to be distinguished from the Ga-H dangling bond configuration on a defect-free hydrogen-covered surface, which has an energy below the valence band edge [14,39,41]. The Ga-H bridge bond can hence be anticipated to be in the lower part of the band gap. Therefore, we suggest that the pinning on p-type hydrogen-exposed surfaces arises from the Ga-H bridge bonds within the As vacancies, with a charge-transfer level $(+/0)$ at $(E_V + 0.25) \pm 0.1$ eV.

Next, we turn to n-type GaAs(110). The dominating defects here are the vacancy-hydrogen complexes. For the Fermi level pinning at $E_V + 0.3$ eV we now need to consider the highest charge-transfer level in the band gap. In order to provide this upward band bending, one needs to have negative surface charges. This can only be achieved by a $(0/-)$ charge-transfer level. If we consider the As vacancy–hydrogen complex with one hydrogen, the addition of a further electron to a neutral defect complex cannot take place in the fully occupied Ga-H bridge bond, but rather needs to be inserted into the Ga-Ga bond, breaking it. This would result in a double-occupied Ga dangling bond, which has almost the same electronic configuration as a Ga-H bridge bond and can hence be expected to have similar charge-transfer levels.

If we consider the As vacancy–hydrogen complex with two hydrogen atoms, again no electron is anticipated to be inserted in the fully occupied Ga-H bridge bonds, but it is conceivable that the additional electron is inserted in the broken

back bond, resulting again in a double-occupied Ga dangling bond, which again can be expected to have similar charge-transfer levels. This defect molecule–based understanding is corroborated by the almost identical charge-transfer levels observed on hydrogen-exposed *p*- and *n*-type GaAs(110) of $(E_V + 0.35) \pm 0.1$ eV and $(E_V + 0.3) \pm 0.1$ eV, respectively. Note that with a detailed theoretical modeling using DFT with the *GW* approximation of the exact defect states of the different vacancy-hydrogen complexes, the locations of electrons could be assessed reliably, but this is outside the scope of the present work.

V. CONCLUSION

The initial stages of hydrogen adsorption on GaAs(110) surfaces have been investigated using atomically resolved scanning tunneling microscopy and spectroscopy. A phase separation into 1×1-reconstructed fully hydrogen-covered and hydrogen-free domains is observed. In the fully hydrogen-covered areas, hydrogen bonds simultaneously to As- and Ga-derived dangling bonds, debuckling and passivating the GaAs(110) surface. At the same time, a high density of hydrogen-etching-induced point defects occur with increasing hydrogen exposure. The dominating defects consist of As vacancy–hydrogen defect complexes, whose Ga-H bridge bonds and double-occupied Ga dangling bonds are suggested to be at the origin of the observed surface Fermi level pinning 0.25 to 0.3 eV above the valence band edge identical within error margins for *p*- and *n*-doped GaAs(110).

ACKNOWLEDGMENT

The authors thank the Deutsche Forschungsgemeinschaft (DFG; German Research Foundation), Project No. 390247238, for financial support.

[1] E. L. McClure, K. L. Schulte, J. Simon, W. Metaferia, and A. J. Ptak, Appl. Phys. Lett. **116**, 182102 (2020).
[2] T. Hannappel, W. McMahon, and J. Olson, J. Cryst. Growth **272**, 24 (2004).
[3] E. Hilner, U. Håkanson, L. E. Fröberg, M. Karlsson, P. Kratzer, E. Lundgren, L. Samuelson, and A. Mikkelsen, Nano Lett. **8**, 3978 (2008).
[4] D. B. Fenner, D. K. Biegelsen, and R. D. Bringans, J. Appl. Phys. **66**, 419 (1989).
[5] M. Herman, W. Richter, and H. Sitter, *Epitaxy* (Springer, Berlin, Heidelberg, 2004).
[6] D. Eaglesham, F. Unterwald, H. Luftman, D. Adams, and S. Yalisove, J. Appl. Phys. **74**, 6615 (1993).
[7] M. Sanchez-Garcia, E. Calleja, E. Monroy, F. Sanchez, F. Calle, E. Muñoz, and R. Beresford, J. Cryst. Growth **183**, 23 (1998).
[8] E. Plis, P. Rotella, S. Raghavan, L. R. Dawson, S. Krishna, D. Le, and C. P. Morath, Appl. Phys. Lett. **82**, 1658 (2003).
[9] R. Sittig, C. Nawrath, S. Kolatschek, S. Bauer, R. Schaber, J. Huang, P. Vijayan, P. Pruy, S. L. Portalupi, M. Jetter, and P. Michler, Nanophotonics **11**, 1109 (2022).
[10] M. Heiss, Y. Fontana, A. Gustafsson, G. Wüst, C. Magen, D. D. O'Regan, J. W. Luo, B. Ketterer, S. Conesa-Boj, A. V. Kuhlmann, J. Houel, E. Russo-Averchi, J. R. Morante, M. Cantoni, N. Marzari, J. Arbiol, A. Zunger, R. J. Warburton, and A. Fontcuberta i Morral, Nat. Mater. **12**, 439 (2013).
[11] A. M. Munshi, D. L. Dheeraj, V. T. Fauske, D. C. Kim, J. Huh, J. F. Reinertsen, L. Ahtapodov, K. D. Lee, B. Heidari, A. T. J. van Helvoort, B. O. Fimland, and H. Weman, Nano Lett. **14**, 960 (2014).
[12] R. B. Lewis, P. Corfdir, J. Herranz, H. Küpers, U. Jahn, O. Brandt, and L. Geelhaar, Nano Lett. **17**, 4255 (2017).
[13] U. del Pennino, C. Mariani, A. Amoddeo, F. Proix, and C. Sébenne, Phys. B: Condens. Matter **170**, 487 (1991).
[14] L. Sorba, M. Pedio, S. Nannarone, S. Chang, A. Raisanen, A. Wall, P. Philip, and A. Franciosi, Phys. Rev. B **41**, 1100 (1990).
[15] F. Proix, Phys. B: Condens. Matter **170**, 457 (1991).
[16] C. Bertoni, F. Finocchi, F. Bernardini, and M. Nardelli, Phys. B: Condens. Matter **170**, 429 (1991).
[17] O. M'Hamedi, F. Proix, and C. Sébenne, Semicond. Sci. Technol. **2**, 418 (1987).
[18] T. Kampen, L. Koenders, K. Smit, M. Rückschloss, and W. Mönch, Surf. Sci. **242**, 314 (1991).
[19] O. Pulci, M. Palummo, A. J. Shkrebtii, G. Onida, and R. Del Sole, Phys. Status Solidi A **175**, 71 (1999).
[20] M. Henzler, Surf. Sci. **22**, 12 (1970).
[21] J. R. Chelikowsky, S. G. Louie, and M. L. Cohen, Phys. Rev. B **14**, 4724 (1976).
[22] D. G. Welkie and M. G. Lagally, J. Vac. Sci. Technol. **16**, 784 (1979).
[23] J. L. A. Alves, J. Hebenstreit, and M. Scheffler, Phys. Rev. B **44**, 6188 (1991).
[24] P. Ebert, Surf. Sci. Rep. **33**, 121 (1999).
[25] J. F. Zheng, X. Liu, N. Newman, E. R. Weber, D. F. Ogletree, and M. Salmeron, Phys. Rev. Lett. **72**, 1490 (1994).
[26] C. Domke, P. Ebert, M. Heinrich, and K. Urban, Phys. Rev. B **54**, 10288 (1996).
[27] S. Landrock, Ph.D. thesis, RWTH Aachen, D 82, Berichte des Forschungszentrums Jülich 4290, 2009.
[28] Domke, Ph.D. thesis, RWTH Aachen, D 82, Berichte des Forschungszentrums Jülich 3566, 1998.
[29] M. Simon, Ph.D. thesis, RWTH Aachen, D 82, Berichte des Forschungszentrums Jülich 3266, 1996.
[30] R. M. Feenstra, J. A. Stroscio, J. Tersoff, and A. P. Fein, Phys. Rev. Lett. **58**, 1192 (1987).
[31] G. Lengel, R. Wilkins, G. Brown, M. Weimer, J. Gryko, and R. E. Allen, Phys. Rev. Lett. **72**, 836 (1994).
[32] P. Ebert, K. Urban, and M. G. Lagally, Phys. Rev. Lett. **72**, 840 (1994).
[33] P. Ebert, K. Urban, L. Aballe, C. H. Chen, K. Horn, G. Schwarz, J. Neugebauer, and M. Scheffler, Phys. Rev. Lett. **84**, 5816 (2000).
[34] P. Ebert, M. Heinrich, M. Simon, K. Urban, and M. G. Lagally, Phys. Rev. B **51**, 9696 (1995).

[35] A. Ruocco, S. Nannarone, M. Sauvage-Simkin, N. Jedrecy, R. Pinchaux, and A. Waldhauer, Surf. Sci. **307**, 662 (1994).
[36] J. Fritsch, A. Eckert, P. Pavone, and U. Schröder, J. Phys.: Condens. Matter **7**, 7717 (1995).
[37] C. Eckl, R. Honke, J. Fritsch, P. Pavone, and U. Schröder, Z. Phys. B **104**, 715 (1997).
[38] S. Nannarone and M. Pedio, Surf. Sci. Rep. **51**, 1 (2003).
[39] A. Wright, C. Fong, and I. P. Batra, Surf. Sci. **244**, 51 (1991).
[40] P. E. Gregory and W. Spicer, Surf. Sci. **54**, 229 (1976).
[41] A. Plesanovas, A. Castellani Tarabini, I. Abbati, S. Kaciulis, G. Paolicelli, L. Pasquali, A. Ruocco, and S. Nannarone, Surf. Sci. **307-309**, 890 (1994).
[42] C. Bertoni, M. Buongiorno Nardelli, F. Bernardini, F. Finocchi, and E. Molinari, Europhys. Lett. **13**, 653 (1990).
[43] G. Cox, D. Szynka, U. Poppe, K. H. Graf, K. Urban, C. KisielowskiKemmerich, J. Krüger, and H. Alexander, J. Vac. Sci. Technol. B **9**, 726 (1991).
[44] M. Heinrich, P. Ebert, M. Simon, K. Urban, and M. G. Lagally, J. Vac. Sci. Technol. A **13**, 1714 (1995).
[45] C. W. M. Castleton, A. Höglund, M. Göthelid, M. C. Qian, and S. Mirbt, Phys. Rev. B **88**, 045319 (2013).
[46] W. Mokwa, D. Kohl, and G. Heiland, Phys. Rev. B **29**, 6709 (1984).
[47] S. Gaan, R. Feenstra, P. Ebert, R. Dunin-Borkowski, J. Walker, and E. Towe, Surf. Sci. **606**, 28 (2012).
[48] M. Heinrich, C. Domke, P. Ebert, and K. Urban, Phys. Rev. B **53**, 10894 (1996).
[49] P. Ebert, M. Heinrich, M. Simon, C. Domke, K. Urban, C. K. Shih, M. B. Webb, and M. G. Lagally, Phys. Rev. B **53**, 4580 (1996).
[50] K.-J. Chao, A. R. Smith, and C.-K. Shih, Phys. Rev. B **53**, 6935 (1996).
[51] C. Domke, P. Ebert, and K. Urban, Phys. Rev. B **57**, 4482 (1998).
[52] L. J. Whitman, J. A. Stroscio, R. A. Dragoset, and R. J. Celotta, Phys. Rev. B **42**, 7288 (1990).
[53] L. J. Whitman, J. A. Stroscio, R. A. Dragoset, and R. J. Celotta, J. Vac. Sci. Technol. B **9**, 770 (1991).
[54] M. Schnedler, V. Portz, P. H. Weidlich, R. E. Dunin-Borkowski, and P. Ebert, Phys. Rev. B **91**, 235305 (2015).
[55] M. Schnedler, R. E. Dunin-Borkowski, and P. Ebert, Phys. Rev. B **93**, 195444 (2016).
[56] J. Bono and R. Good, Surf. Sci. **175**, 415 (1986).
[57] R. Feenstra and J. Stroscio, J. Vac. Sci. Technol. B **5**, 923 (1987).
[58] M. Hedström, A. Schindlmayr, G. Schwarz, and M. Scheffler, Phys. Rev. Lett. **97**, 226401 (2006).
[59] S. B. Zhang and A. Zunger, Phys. Rev. Lett. **77**, 119 (1996).
[60] H. Kim and J. R. Chelikowsky, Phys. Rev. Lett. **77**, 1063 (1996).
[61] H. Kim and J. R. Chelikowsky, Surf. Sci. **409**, 435 (1998).